Class-II neurons display a higher degree of stochastic synchronization than class-I neurons

Sashi Marella*
Center for Neuroscience, University of Pittsburgh, Pittsburgh, Pennsylvania, 15261 USA

G. Bard Ermentrout†
Department of Mathematics/Statistics, University of Pittsburgh, Pittsburgh, Pennsylvania, 15261 USA
(Received 11 January 2008; published 29 April 2008)

We describe the relationship between the shape of the phase-resetting curve (PRC) and the degree of stochastic synchronization observed between a pair of uncoupled general oscillators receiving partially correlated Poisson inputs in addition to inputs from independent sources. We use perturbation methods to derive an expression relating the shape of the PRC to the probability density function (PDF) of the phase difference between the oscillators. We compute various measures of the degree of synchrony and cross correlation from the PDF's and use the same to compare and contrast differently shaped PRCs, with respect to their ability to undergo stochastic synchronization. Since the shape of the PRC depends on underlying dynamical details of the oscillator system, we utilize the results obtained from the analysis of general oscillator systems to study specific models of neuronal oscillators. It is shown that the degree of stochastic synchronization is controlled both by the firing rate of the neuron and the membership of the PRC (type I or type II). It is also shown that the circular variance for the integrate and fire neuron and the generalized order parameter for a hippocampal interneuron model have a nonlinear relationship to the input correlation.

DOI: 10.1103/PhysRevE.77.041918 PACS number(s): 87.18.Sn, 84.35.+i, 05.10.Gg

I. INTRODUCTION

There has recently been a great deal of interest in the ability of noise to synchronize limit-cycle oscillators even when they are uncoupled [1–8]. Two uncoupled limit-cycle oscillators driven by partially or fully correlated noise that is not too strong are able to synchronize in the sense that their phase difference approaches a stationary distribution peaked around zero. Goldobin *et al.* [3] and more recently, Nakao *et al.* [9] derived expressions for the density of phase differences when oscillators are driven by partially correlated white noise. In recent experiments, Galan *et al.* [10] showed partial synchronization of two olfactory bulb neurons when driven by partially correlated synaptic events. If this so-called stochastic synchronization plays a role in biological networks, then it would be useful to quantitatively characterize the consequences of uncorrelated signals and oscillator heterogeneity as a function of the details of the oscillators. For small noise levels, it has been shown [2,3,9] (for white noise stimuli) that a general limit-cycle oscillator can be reduced to a scalar equation for the phase characterized by the phase-resetting curve (or PRC). The PRC of an oscillator describes how the timing of a brief signal changes the phase of the oscillator. PRCs are easily measured experimentally and computed numerically for a given model.

Neural and other biological oscillators can be classified broadly into two types based on their intrinsic dynamics [11]. That is, as a parameter changes (e.g., the injected current in a neuron), the system goes from a stable rest state to periodic firing through a bifurcation; two such bifurcations characterize the majority of tonically spiking neurons. Class-I excitable neurons undergo *saddle-node on invariant circle* bifurcations and can theoretically fire at arbitrarily low finite frequencies whereas class-II excitable neurons undergo either *subcritical* or *supercritical Andronov-Hopf* bifurcations and possess a nonzero minimum frequency of firing. Ermentrout and collaborators [12,13], Hansel *et al.* [14], and more recently, Brown *et al.* [15] have demonstrated that there is a strong connection between the bifurcation class of a neuron and the shape of its phase-resetting curve. Class-I excitable neurons, at least near the bifurcation, tend to have PRCs which are non-negative; inputs can only advance the phase [16]. Class-II excitable neurons tend to have PRCs which have both positive and negative parts [16]. Thus for class-II excitable neurons, the next spike is advanced or delayed depending on the timing of the subthreshold input. The shape of the PRC plays an important role in determining whether coupled neurons are able to synchronize both in models [12,13,17–19] and in experimentally manipulated neurons [20–22]. Thus, we expect that the shape of a neural PRC might also factor in the degree of stochastic synchronization to noise. Recently, Tateno and Robinson [23,24] used the phase-resetting curve of both model neurons and cortical neurons to study how the shape of the PRC affects the rate that two identical neurons driven by perfectly correlated noise can synchronize. Galan *et al.* [25] used finite element method to contrast the stochastic synchronization of class-I and class-II neurons to white noise. Interestingly, Tsubo *et al.* [26] show that the shape of the PRCs is different in different layers of the rat motor cortex.

In this paper, we first derive an expression for the density of phase differences for two identical oscillators driven by partially correlated Poisson inputs. It turns out that in the limit of small perturbations, we obtain a result identical to Nakao's recent calculation [9]. Secondly, we explore how the shape of the PRC impacts the relationship between the input

*Also at Center for the Neural Basis of Cognition, Carnegie Mellon University.
†bard@math.pitt.edu; URL: http://www.pitt.edu/~phase

correlation and synchrony of driven oscillators. Finally, we explore the effects of the oscillator frequency on stochastic synchrony as it is known [13] that frequency has a strong effect on the shape of the PRC.

II. DERIVATIONS

A. Reduction to a phase equation

Consider a general limit-cycle oscillator that is driven by an input,

$$\frac{dX}{dt} = F(X(t)) + G(X(t),t).$$

When $G=0$, we have a stable periodic solution, $X_0(t)$. As in Kuramoto [27], we can introduce a phase variable along limit cycle θ so that we write $X(t)=X_0(\theta(t))$ and obtain

$$\frac{d\theta}{dt} = 1 + Z(\theta(t)) \cdot G(X_0(\theta(t)),t)$$

as long as G is small (which is the case we consider here). The vector function $Z(\theta)$ describes the phase shift of the oscillator as a function of the timing (phase) of the stimulus. Now suppose that $X(t)$ is a neural oscillator which is driven by a series of pulsatile inputs with amplitude a_m at times $t_1, t_2, \ldots$. Since the drive only appears in the voltage variable, only the voltage component of $Z(\theta)$ matters; this is the infinitesimal phase-resetting curve $\Delta(\theta)$ for the neuron. Thus the phase satisfies

$$\frac{d\theta}{dt} = 1 + \sum_m \Delta(\theta(t)) a_m \delta(t - t_m).$$

Let $\tau_m = t_m - t_{m-1}$ be the time between impulses. Between inputs, the phase (measured in units of time) advances by τ_m. If we let θ_m be the phase right before the mth stimulus, then

$$\theta_{m+1} = \theta_m + \tau_m + a_m \Delta(\theta_m). \tag{1}$$

We note that θ lies between $[0,T)$, where T is the natural period of the oscillator. We now have reduced the driven oscillator to a one-dimensional map. If the pulsatile stimuli are not delta functions but rather some type of brief synaptic current, then the map derivation can be valid (or certainly a good approximation) when the PRC is replaced by another quantity called the spike-time response curve (STRC). For example, if the inputs are time-dependent functions, say, $i(t)$, then the PRC is replaced by

$$\Delta_i(\theta) = \int_0^\infty \Delta(\theta - \theta') i(\theta') d\theta'.$$

With regular inputs, this replacement is valid as long as $i(t)$ lasts for a short time compared to the interstimulus interval. However, for Poisson inputs, the interstimulus interval can be arbitrarily short, so that using an STRC may not be formally legitimate.

Experimentally, the function $\Delta(\theta)$ is obtained by perturbing the oscillator with small stimuli (say, amplitude a) and measuring the change in the spike time as follows:

$$\hat{\Delta}(t,a) \equiv T - T_{pert}(t,a).$$

The function $\Delta(t)$ is defined as

$$\Delta(t) = \lim_{a \to 0} \frac{\hat{\Delta}(t,a)}{a}.$$

It is called the *infinitesimal* PRC. For numerically computed oscillations, $\Delta(t)$ is found by solving the adjoint equation, a linear equation associated with the limit-cycle solution [28].

B. Phase distribution equation

We first consider the invariant phase of a single perturbed oscillator. If τ_m are taken from a distribution $Q(\tau)$ $(\tau \in [0,T))$ and a_m are taken from a distribution with density, $f(a)$, then we can readily derive an equation for the density of phases θ_m in Eq. (1) using methods of Lasota and Mackey [29]. Let $P_m(\theta)$ be the density of θ_m. Then

$$P_{m+1}(\theta) = \int_{-\infty}^{\infty} \int_0^T P_m(y) Q(\theta - y - a\Delta(y)) f(a) dy\, da.$$

A number of authors have analyzed this model when $f(a)$ is strongly peaked near $a=0$, e.g., stimuli are weak; or when the Poisson rate is very fast. Nakao *et al.* [30] and Ermentrout *et al.* [31] show that to lowest order, the invariant density $\varphi(\theta) \equiv P_\infty(\theta)$ is very close to uniform, $\varphi(\theta) \approx 1/T$. We will show later, that formally, we have to make a small correction even for weak inputs, but for Poisson inputs at low rates, the results are indistinguishable from those obtained by treating $\varphi(\theta)$ as uniform. For notational simplicity, we will assume that the period T has been scaled to 1. Consider, now, N identical uncoupled oscillators, driven with pulsatile stimuli that are only partially shared. That is, at any given moment, some oscillators will receive a perturbation, but others will not. Our goal is to study how synchronous the oscillators are as a function of the degree of sharing. As the oscillators are uncoupled, it suffices to analyze a pair. Thus, consider two such oscillators with identical periods as follows:

$$\Theta_{n+1} = \Theta_n + \tau_n + \epsilon a_n \Delta(\Theta_n), \tag{2}$$

$$\Psi_{n+1} = \Psi_n + \tau_n + \epsilon b_n \Delta(\Psi_n), \tag{3}$$

where Θ and Ψ denote the phase of the oscillators at the time of the nth input. τ_n is the period of stimulation; specifically, it is the time between the nth and the $n+1$th inputs and is assumed here to be a Poisson variable. The parameter ϵ scales the magnitude of the perturbations. We allow for heterogeneity in the inputs; some inputs are shared while others are not. The easiest way to do this is to assume that a_n, b_n are either 0 or 1: $(a_n, b_n) \in \{(1,1),(0,1),(1,0)\}$ with probabilities $q, (1-q)/2$ and $(1-q)/2$, respectively. Thus, q is the probability that both oscillators receive the same input and thus is related to the correlation of the inputs. In Appendix A we show that the correlation is $c := 2q/(q+1)$. Additional heterogeneity could come via small differences in the frequencies of the oscillators. At the end of the derivation, we discuss this point briefly. We assume Δ to be a periodic func-

tion with period 1. The phase difference of the oscillators at the time of the $n+1$th input, $\delta_n=\Theta_n-\Psi_n$ can be obtained by subtracting Eq. (3) from Eq. (2).

$$\delta_{n+1} = \delta_n + \epsilon(a_n\Delta(\delta_n+\Psi_n) - b_n\Delta(\Psi_n)).$$

In order to analyze these equations, we will derive an equation for the density of δ_n using methods for stochastic maps in [29]. We note that Ψ_n are random variables which are independent of δ_n and furthermore, that a_n and Ψ_n are independent as well since Ψ_n depends only on a_{n-1}. Thus, given the probabilities of a_n, b_n, and Ψ_n, we can compute the evolution of the density for δ_n and thus the invariant density.

Let $p_n(x)dx := \Pr(\delta_n \in [x, x+dx))$, that is, $p_n(x)$ is the density function for the phase difference δ_n. With some abuse of notation, we will suppress the dx, first on the right-hand side and later on the left-hand side of the definition. Let

$$E[U(\Psi)] := \int_0^1 U(\Psi)\varphi(\Psi)d\Psi,$$

where U is an arbitrary function of Ψ and $\varphi(\Psi)$ is the invariant density for Ψ_n. Henceforth, we drop the subscript n from Ψ_n

$$\begin{aligned} p_{n+1}(x)dx &= E[\Pr(\delta_n + \epsilon a_n\Delta(\delta_n+\Psi) - \epsilon b_n\Delta(\Psi) = x)] \\ &= qE[p_n^{11}(x,\Psi)dx] + \left(\frac{1-q}{2}\right)(E[p_n^{01}(x,\Psi)dx] \\ &\quad + E[p_n^{10}(x,\Psi)dx]), \end{aligned}$$

where $p_{n+1}^{ab}(x,\Psi)dx$ is the probability that $\delta_{n+1}=x$ given (a,b) and Ψ. We now compute all the $p_n^{ab}(x,\Psi)dx$ quantities.

$$\begin{aligned} p_n^{01}(x,\Psi)dx &= \Pr(\delta_n - \epsilon\Delta(\Psi) = x) \\ &= \Pr(\delta_n = \epsilon\Delta(\Psi) + x) = p_n(\epsilon\Delta(\Psi)+x)dx. \end{aligned}$$

Before continuing, we define $F(x) := x+\epsilon\Delta(x)$. For ϵ sufficiently small, $F(x)$ is an invertible function.

$$\begin{aligned} p_n^{10}(x,\Psi)dx &= \Pr(\delta_n + \epsilon\Delta(\delta_n+\Psi) = x) \\ &= \Pr(\delta_n + \Psi + \epsilon\Delta(\delta_n+\Psi) = x+\Psi) \\ &= \Pr(F(\delta_n+\Psi) = x+\Psi) \\ &= \Pr(\delta_n = F^{-1}(x+\Psi) - \Psi). \end{aligned}$$

Since

$$\begin{aligned} \Pr(\delta_n + \epsilon\Delta(\delta_n+\Psi) \le x) &= \Pr(F(\delta_n+\Psi) - \Psi \le x) \\ &= \Pr(\delta_n \le F^{-1}(x+\Psi) - \Psi). \end{aligned}$$

We can write,

$$\begin{aligned} p_n^{10}(x,\Psi) &= \frac{d}{dx}\int_0^x p_n^{10}(s,\Psi)ds \\ &= \frac{d}{dx}\int_0^{F^{-1}(x+\Psi)-\Psi} p_n(s,\Psi)ds \\ &= p_n(F^{-1}(x+\Psi)-\Psi,\Psi)\frac{d}{dx}(F^{-1}(x+\Psi)-\Psi) \\ &= \frac{p_n(F^{-1}(x+\Psi)-\Psi,\Psi)}{F'(F^{-1}(x+\Psi))}. \end{aligned}$$

Hence,

$$p_n^{10}(x,\Psi)dx = \frac{p_n(F^{-1}(x+\Psi)-\Psi,\Psi)dx}{F'(F^{-1}(x+\Psi))}.$$

Lastly,

$$\begin{aligned} p_n^{11}(x,\Psi)dx &= \Pr(\delta_n + \epsilon(\Delta(\delta_n+\Psi) - \Delta(\Psi)) = x) \\ &= \Pr(\delta_n + \Psi + \epsilon\Delta(\delta_n+\Psi) = x + \Psi + \epsilon\Delta(\Psi)) \\ &= \Pr(F(\delta_n+\Psi) = x + F(\Psi)) \\ &= \Pr(\delta_n = F^{-1}(x+F(\Psi)) - \Psi) \\ &= \frac{p_n\,(F^{-1}(x+F(\Psi))-\Psi),\Psi)dx}{F'(F^{-1}(x+F(\Psi)))}. \end{aligned}$$

Thus, $p_n(x)$ satisfies the Frobenius-Perron equation

$$\begin{aligned} p_{n+1}(x) = \int_0^1 \varphi(\Psi)qp_n^{11}(x,\Psi)dx + \left(\frac{1-q}{2}\right)[p_n^{10}(x,\Psi)dx \\ + p_n^{01}(x,\Psi)dx]d\Psi. \end{aligned}$$

The invariant (steady-state) density is found by equating $p_n(x)$ and $p_{n+1}(x)$, thus we need to solve

$$\begin{aligned} p(x) = \int_0^1 \varphi(\Psi)\left[q\left(\frac{pF^{-1}(x+F(\Psi)-\Psi))}{F'(F^{-1}(x+F(\Psi)))}d\Psi\right) + \left(\frac{1-q}{2}\right)\right. \\ \left.\times\left(\frac{p(F^{-1}(x+\Psi)-\Psi))}{F'(F^{-1}(x+\Psi))} + p(\Delta(\Psi)+x)\right)\right]. \end{aligned} \tag{4}$$

In order to analyze Eq. (4), we need to know the distribution of the phase $\varphi(\Psi)$. As noted at the beginning of this section, if the stimuli are small, that is, $\epsilon \ll 1$, then $\varphi(\Psi)\approx 1$; it is very close to uniform. In this case, the integrals in Eq. (4) are simple averages. However, as our calculations for the invariant density $p(x)$ require $O(\epsilon^2)$ terms, we have to compute $\varphi(\Psi)$ up to order ϵ. The uniform approximation has been used in other papers, but, strictly speaking, we need to include the next order terms. As we will see later on, the higher order terms in $\varphi(\Psi)$ make almost no difference for Poisson inputs at low rates. In Appendix B, we derive the expression for $\varphi(\Psi)$ for Poisson inputs with rate r as follows:

$$\varphi(\Psi) = 1 - \epsilon\left(r\frac{1+q}{2}(\Delta(\Psi)-\bar{\Delta})\right), \tag{5}$$

where $\bar{\Delta}$ is the average of $\Delta(\Psi)$.

Now, let $y=F(x)=x+\epsilon\Delta(x)$ and express x approximately in terms of y

$$\begin{aligned} x &\approx y + \epsilon y_1 + \epsilon^2 y_2 \\ &\Rightarrow F(x) = x + \epsilon\Delta(x) \\ &\approx y + \epsilon y_1 + \epsilon^2 y_2 + \epsilon\Delta(y + \epsilon y_1 + \epsilon^2 y_2). \end{aligned}$$

By Taylor expansion of $\epsilon\Delta(y+\epsilon y_1+\epsilon^2 y_2)$ around y we get

$$\epsilon\Delta(y+\epsilon y_1+\epsilon^2 y_2)\approx \epsilon\Delta(y)+\epsilon^2\Delta'(y)y_1+O(\epsilon^3)$$
$$\Rightarrow F(x)\approx y+\epsilon y_1+\epsilon^2 y_2+\epsilon\Delta(y)+\epsilon^2\Delta'(y)y_1.$$

Equating the ϵ terms we can solve for y_1 and y_2 obtaining the inverse to second order as follows:

$$x=F^{-1}(y)\approx y-\epsilon\Delta(y)+\epsilon^2\Delta'(y)\Delta(y). \tag{6}$$

We use the result in Eq. (6) to express terms in Eq. (4) in terms of their expansion in ϵ. For example, a term such as $p(F'(F^{-1}(g)))$ [which does not appear in Eq. (4)] can be expressed using Eq. (6) as

$$p(F'(F^{-1}(g)))=p(1+\epsilon\Delta'(x(g-\epsilon\Delta g)+\epsilon^2\Delta' g\Delta g)),$$

leading to

$$p(1)+\epsilon p'(1)\Delta'(g)+\epsilon^2\left(-p'(1)\Delta''(g)\Delta(g)+\frac{1}{2}p''(1)\Delta(g)^2\right)+O(\epsilon^3).$$

Using the above scheme, Eq. (4) can be expressed as

$$p(x)=\int_0^1[1+\epsilon\varphi_1(\Psi)]\Bigg[q\Bigg[p(x)+\epsilon(-p'(x)(-\Delta(\Psi)+\Delta(x+\Psi))-p(x)\Delta'(x+\Psi))+\epsilon^2\Bigg(-p'(x)\Delta'(x+\Psi)\Delta(\Psi)+p'(x)$$
$$\times\Delta'(x+\Psi)\Delta(x+\Psi)+\frac{1}{2}p''(x)(\Delta(\Psi))^2-p''(x)\Delta(\Psi)\Delta(x+\Psi)+\frac{1}{2}p''(x)(\Delta(x+\Psi))^2+p(x)\Delta''(x+\Psi)(-\Delta(\Psi)$$
$$+\Delta(x+\Psi))+(-p'(x)\Delta(\Psi)+p'(x)\Delta(x+\Psi)+p(x)\Delta'(x+\Psi))\Delta'(x+\Psi)\Bigg)+O(\epsilon^3)\Bigg]+\frac{1-q}{2}\Bigg[p(x)+\epsilon(-p'(x)\Delta(x+\Psi)$$
$$-p(x)\Delta'(x+\Psi))+\epsilon^2\Bigg(p'(x)\Delta'(x+\Psi)\Delta(x+\Psi)+\frac{1}{2}p''(x)(\Delta(x+\Psi))^2+p(x)\Delta''(x+\Psi)\Delta(x+\Psi)+(p'(x)\Delta(x+\Psi)$$
$$+p(x)\Delta'(x+\Psi))\Delta'(x+\Psi)\Bigg)+O(\epsilon^3)\Bigg]+\frac{1-q}{2}\Bigg[p(x)+\epsilon p'(x)\Delta(\Psi)+\frac{1}{2}\epsilon^2 p''(x)(\Delta(\Psi))^2+O(\epsilon^3)\Bigg]\Bigg]d\Psi.$$

To lowest order, we get

$$p(x)=\int_0^1 p(x)d\Psi=p(x).$$

To order ϵ, we obtain

$$0=qp(x)\int_0^1\varphi_1(\Psi)d\Psi+\frac{q+1}{2}\int_0^1 p'(x)\Delta(\Psi)-p'(x)\Delta(x+\Psi)-p(x)\Delta'(x+\Psi)d\Psi.$$

Since $\varphi(\Psi)$ is the invariant density, by definition $\int_0^1\varphi(\Psi)d\Psi=1$. Hence $\int_0^1\varphi_1(\Psi)d\Psi=0$, where φ_1 is the first-order ϵ term in the expansion of $\varphi(\Psi)$ (see Appendix B). Hence we can write

$$0=\frac{q+1}{2}\int_0^1 p'(x)\Delta(\Psi)-p'(x)\Delta(x+\Psi)-p(x)\Delta'(x+\Psi)d\Psi.$$

Using the periodicity of $\Delta(\Psi)$, we observe that the right-hand side is zero independent of $p(x)$. Henceforth, we denote $p(x)$ as p for reasons of brevity. To second order we must have

$$0=\int_0^1\Bigg(-4qp'\Delta'(x+\Psi)\Delta(\Psi)+2qp'\Delta'(x+\Psi)\Delta(x+\Psi)+\frac{1}{2}qp''\Delta^2(\Psi)-2qp''\Delta(\Psi)\Delta(x+\Psi)+\frac{1}{2}qp''\Delta^2(x+\Psi)$$
$$-2qp\Delta''(x+\Psi)\Delta(\Psi)+qp\Delta''(x+\Psi)\Delta(x+\Psi)+qp\Delta'(x+\Psi)^2+2p'\Delta'(x+\Psi)\Delta(x+\Psi)+\frac{1}{2}p''\Delta^2(x+\Psi)$$
$$+p\Delta''(x+\Psi)\Delta(x+\Psi)+p\Delta'(x+\Psi)^2+\frac{1}{2}p''\Delta^2(\Psi)\Bigg)d\Psi-\int_0^1 r\left(\frac{q+1}{2}\right)^2[\Delta(\Psi)-\bar{\Delta}][(p\Delta(\Psi)-p'\Delta(x+\Psi)$$
$$-p\Delta'(x+\Psi))d\Psi]. \tag{7}$$

The second integral arises as a consequence of the order ϵ terms in the density function $\varphi(\Psi)$. Let us define

$$h(x) := \int_0^1 \Delta(\Psi)\Delta(\Psi + x)d\Psi,$$

and observe the following:

$$\int_0^1 \Delta(\Psi)d\Psi = \int_0^1 \Delta(x + \Psi)d\Psi,$$

$$\int_0^1 \Delta''(\Psi)\Delta(\Psi)d\Psi = -\int_0^1 \Delta'(\Psi)^2 d\Psi.$$

With these definitions, observations, and the fact that $\Delta(\Psi)$ is periodic, we can simplify Eq. (7) to

$$0 = -4qp'h'(x) + (1+q)p''h(0) - 2qp''h(x) - 2qph''(x) + r\frac{(q+1)^2}{4}[h'(x)p + (h(x) - h(0))p']. \quad (8)$$

If $G(x) = 1 - \frac{2q}{(1+q)}\frac{h(x)}{h(0)}$ and $H(x) = \frac{(1+q)}{4}(1 - \frac{h(x)}{h(0)})$, then Eq. (8) is equivalent to

$$[p(x)G(x)]'' - r[p(x)H(x)]' = 0. \quad (9)$$

This can be integrated to yield a complex expression for the density function for the phase differences. However, it is much easier to first consider the low rate approximation where $r=0$. Using boundary conditions $p(0)=p(1)$ we can solve for constants C_1 and C_2 in the solution to the second-order differential equation in Eq. (9) as follows:

$$p(x)G(x) = C_1 x + C_2,$$

$$C_1 = 0, \quad C_2 = \frac{1}{\int_0^1 \frac{1}{G(x)}dx},$$

where the condition on C_1 comes from the periodicity of $p(x)$ and the condition on C_2 comes from the normalization of $p(x)$. Thus

$$p(x) = \frac{C_2}{1 - c\frac{h(x)}{h(0)}},$$

where we have substituted $c = 2q/(1+q)$, the value of the input correlation. Thus, for low rate Poisson inputs with a small PRC we obtain exactly the same equation for the density of phase differences as was derived by Nakao *et al.*[9] for the white noise case. We summarize the result as follows. For two identical oscillators with input correlation c and slow Poisson impulses, the density of the phase differences is given by

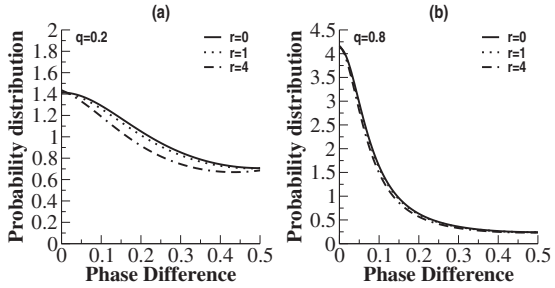

FIG. 1. Steady-state density $p(x)$ for $q=0.2$ and $q=0.8$ with different values of the Poisson rate r.

$$p(x) = \frac{N}{1 - c\frac{h(x)}{h(0)}}, \quad (10)$$

where $h(x)$ is the autocorrelation of the PRC, where N is the normalization term C_2. As $c \to 1$, $p(x) \to \delta(x)$, the Dirac delta function. Thus perfectly correlated noisy oscillators will synchronize with zero phase lag. If $c=0$, then $p(x)=1$ is uniform.

The full equation (9) with $r \neq 0$ can be solved exactly but little intuition can be gained. In Fig. 1, we show the numerical solution to Eq. (9) for two different values of q and for various values of the rate r. At the high value $q=0.8$ corresponding to 80% shared input ($c=8/9$), the effects of the Poisson rate on the shape of the stationary density $p(x)$ are minimal. At lower correlation, e.g., 20% shared input ($c=1/3$), the rate has a stronger effect although it is still quite small. Heterogeneity in the actual frequencies of the two oscillators will contribute a term of the form $(-p(x)\mu)'$ to the left-hand side of Eq. (9), where μ is the difference in the frequencies of the two oscillators. Thus drift will shift the peak of $p(x)$, but will not significantly change the width of the peak. Thus, we will ignore heterogeneity from now on.

In the remainder of the paper, we explore how the shape of the PRC affects the degree of synchronization with partially correlated inputs using the small r approximation (10). Since Eq. (10) is the same as derived in Nakao *et al.* [9], what we conclude about shape and synchrony for Poisson inputs will also hold for white noise.

In order to quantify difference in the shapes of the density, $p(x)$, we need to introduce some measure of the degree of synchrony. We will analyze several different measures. The simplest is

$$z_1 = \int_0^1 \cos(2\pi x)p(x)dx. \quad (11)$$

If $p(x)$ is uniform, then $z_1=0$ and if $p(x)$ is a delta function, $z_1=1$. The *circular variance* or *vector strength* [32] of a distribution on the circle is defined as

$$\mathrm{Var}(\theta) = 1 - R/n,$$

where

$$R^2 = \left(\sum_{j=1}^{n} \cos 2\pi\theta_j\right)^2 + \left(\sum_{j=1}^{n} \sin 2\pi\theta_j\right)^2.$$

Circular variance characterizes phase locking between oscillators. Since $p(x)$ is symmetric for identical oscillators, the sine average of the phases vanishes, and our order parameter is exactly R/n. Thus, the circular variance $1-z_1$ is a good measure of the tightness of the distribution on the circle. For sharp distributions, higher-order circular moments may be a better measure, e.g.,

$$z_j = \int_0^1 \cos(2\pi jx)p(x)dx,$$

since z_1 measures how close $p(x)$ is to a pure cosine curve. We use the first n of order parameters, and take the limit as $n \to \infty$; we obtain a general order parameter, $p(0)-1$ (see Appendix C). A common measure that is used in neuroscience is the cross correlation. However, for this to make sense, we need to map the phase model onto a "spike train." Pfeuty *et al.* [33] consider a simple example $S_j(t)$, defined to be $1/\delta$ if $\theta_j(t)$ is within δ of $\theta=0$ and $S_j(t)=0$ otherwise. They show that the cross correlation of two such spike trains is just $p(x)$, that is,

$$\frac{\langle S_1(t_1)S_2(t_2)\rangle}{\langle S_1(t)\rangle\langle S_2(t)\rangle} = p(t_2 - t_1).$$

Thus, a measure of the degree of synchrony is the peak $p(0)$, which is related to our generalized order parameter. Like that parameter, there is no simple way to normalize this cross correlation.

III. EXAMPLES

A. Comparison with simulations

We first illustrate how well the theory works by comparing Monte Carlo simulations with Eq. (10) and varying the amplitude of the PRC and the rate of the Poisson process. Figure 2 shows an example Monte Carlo simulation of Eqs. (2) and (3) for different Poisson rates and for different PRC amplitudes using a sinusoidal PRC. We iterate 10^6 times and bin the resulting data into 100 bins between −0.5 and 0.5. Over a range of two orders of magnitude in the Poisson rates, there is no difference in the shape of the density function. Similarly, for small amplitudes, there are no differences in the density either. However, if the amplitude becomes large enough, then the approximation of uniformity for the phase of individual oscillators breaks down and Eq. (10) becomes inaccurate. For example, Fig. 2(d) shows the density of the oscillator phase in Eq. (2) as the amplitude of the PRC increases. Finally, with a modest amplitude, Eq. (10) provides a precise approximation of the Monte Carlo histogram as shown in Fig. 2(c).

B. Shape matters

We use the terms "type I" and "type II" to refer to the PRCs of class-I and class-II neurons, respectively, and use $1-\cos(\theta)$ and $\sin(\theta)$ as their respective idealizations. Theo-

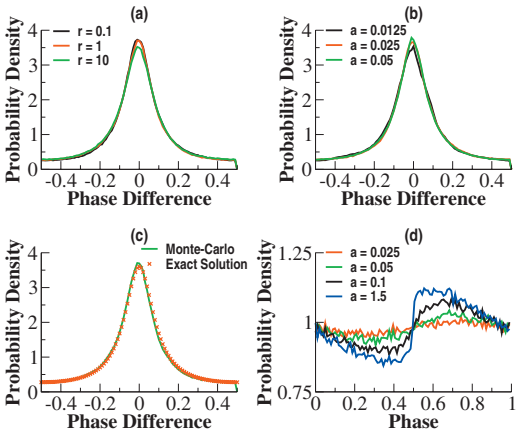

FIG. 2. (Color) Monte Carlo simulations for $\Delta(x)=a \sin 2\pi x$, with $q=0.75$ and Poisson rate r. 10^6 iterations are run and binned in 100 bins on the interval $[-0.5,0.5)$. (a) Independence of the rate for $r=0.1$, 1, 10 at $a=0.025$. (b) Independence of the amplitude for small amplitudes, $a=0.0125$, 0.025, 0.05 at $r=1$. (c) Comparison of the $r=1$, $a=0.025$ case for $q=0.75$ with the density from Eq. (10). (d) Larger amplitudes result in more nonuniformity in the distribution of individual oscillator phases at rate $r=1$.

retical predictions for the probability density functions of phase differences for classical type-I and type-II PRCs can be obtained from Eq. (10). For two sample values of q, we show that type-II oscillators have a narrower distribution of phase differences around zero, compared to type I as can be seen in Fig. 3. Note that both these oscillator types will synchronize at identical rates if $q=1$ since their Lyapunov exponents are the same [2]. Using Eq. (11) we calculated the circular variance of the distribution obtained from Eq. (10). Since physical systems like postsynaptic neurons have to accommodate jitter around a zero difference in the presynaptic spike times, we calculated the probability that the phase difference lies within a 0.2 T interval around zero, i.e., Prob($\delta \in [-0.1,0.1]$). In Fig. 4(b) and all subsequent plots, Prob($\delta \in [-0.1,0.1]$) is plotted after subtracting its value at $q=0$, hence the plot purely reflects the contribution of nonzero q. In Fig. 4(a), it can be seen that the circular variance of the phase differences for type-II oscillators is lower (higher values of the order parameter z_1) than that for type-I oscillators for all possible values of q. In Fig. 4(b), it can be

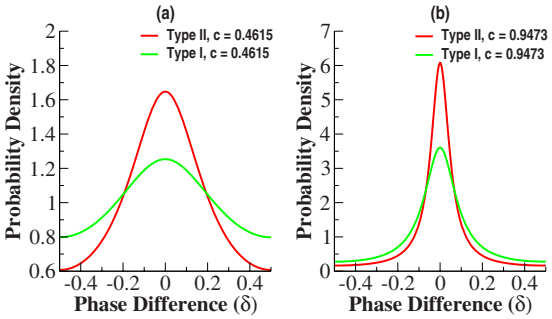

FIG. 3. (Color online) Simulation results showing distribution of phase differences for type-I and type-II PRCs, at two different input correlations ($q=0.3$ and $q=0.9$). Probability is plotted along the ordinate and the phase differences on the abscissa.

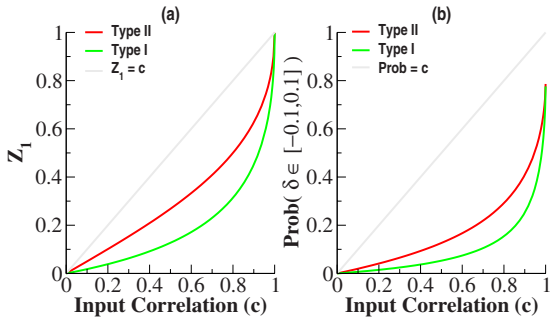

FIG. 4. (Color online) Comparison of the order parameter between type-I and type-II PRCs.

seen that there is a higher probability for type-II oscillators to stay closer in phase than type-I oscillators. We note that choice of the length of the interval is arbitrary and the relationship between the curves is conserved at other choices of interval lengths. Taken together, these three results show that for any given input correlation $c<1$, type-II oscillators have a higher probability of undergoing stochastic synchronization compared to type-I oscillators for nonzero q. This observation supports the hypothesis that the shape of the PRC can determine the degree to which uncoupled oscillators can synchronize under the influence of noise.

For small values of input correlation, c, we can get an approximation for the order parameter as well as the peak of the density function. For c small,

$$p(x) = \frac{N}{1 - ch(x)/h(0)} \approx N(1 + ch(x)/h(0))$$

from which we find that

$$N \approx 1 - c\int_0^1 h(x)/h(0)dx := 1 - c\langle h\rangle/h(0),$$

so that

$$p(0) - 1 \approx c(1 - \langle h\rangle/h(0)).$$

Thus, the peak of the probability distribution function and the generalized order parameter are maximized when the average value of $h(x)$ is zero. Recalling the definition of $h(x)$, we obtain the concise formula for small correlations as follows:

$$p(0) - 1 \approx c\left[1 - \frac{\langle\Delta\rangle^2}{\langle\Delta^2\rangle}\right]. \quad (12)$$

Holding the L_2 *norm* of Δ constant $\sqrt{\langle\Delta^2\rangle}$, we see that the dc component of Δ is what hurts the ability to synchronize at low input correlation. Type-II oscillators have a lower dc component and thus synchronize more readily.

C. Dependence on firing rate

We also investigated the influence of firing rate on stochastic synchronization. PRCs for a model neuron obtained in low and high firing frequency regimes [13] were fit using a polynomial function $x^n(x-1)^m$. Both PRCs were type I, i.e., the membership of the PRC remained type I in both the frequency regimes. Using these fits, we calculated the probability density of the phase differences and 1-circular variance. The results are plotted in Fig. 5. It can be seen that for higher firing rate (corresponding to $n=2$, $m=1$) there is a broader distribution of phase difference around zero and also a higher circular variance (lower values of the order parameter z_1). These results suggest that increase in firing frequency decreases the probability of synchronization due to stochastic input for a type-I PRC.

Firing rate dependence of stochastic synchronization was investigated in another model neuron, specifically the Morris-Lecar (ML) system. The parameters for the model can be tuned such that the model displays either a type-I or type-II PRC. In both these regimes the PRC has a tendency to become more negative with an increase in the input current. For a ML system with a type-I PRC under moderate current conditions, this translates to a conversion from a classic type-I to a type-II PRC. A type-II ML system on the other hand continues to experience an increase in its negative part with an increase in input current. Figure 7 shows a ML system with a type-I PRC. It can be seen that there is narrowing of the distribution of phase differences accompanied by lower circular variance for the system firing at a higher frequency with a type-II PRC. A similar transition can be observed for a ML system with parameters set to a type-II PRC regime (Fig. 7), but the magnitude of change is much less, since the system has a type-II PRC at the outset as can be seen in Figs. 6 and 7.

The leaky integrate and fire (LIF) model is used widely as a first approximation to continuous and realistic neuronal

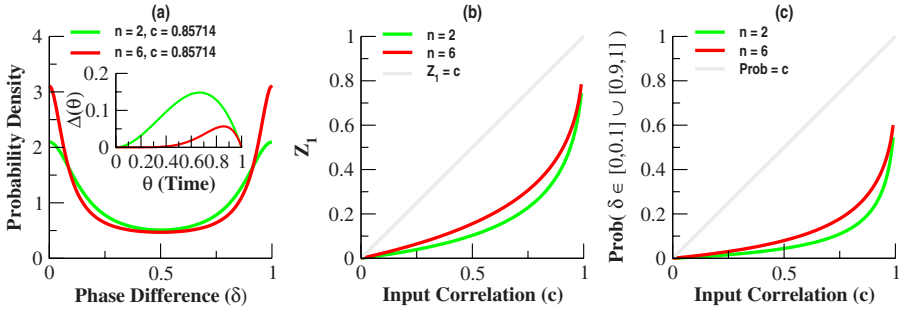

FIG. 5. (Color online) Simulations showing the effect of firing rate on stochastic synchronization. PRCs from Gutkin *et al.* [13] were fit using $x^n(1-x)^m$, where the values of $n=2$, $m=1$ and $n=6$, $m=1$ were used to fit the high and low frequency firing, respectively. The inset in (a) shows PRCs for both frequencies for $q=0.75$.

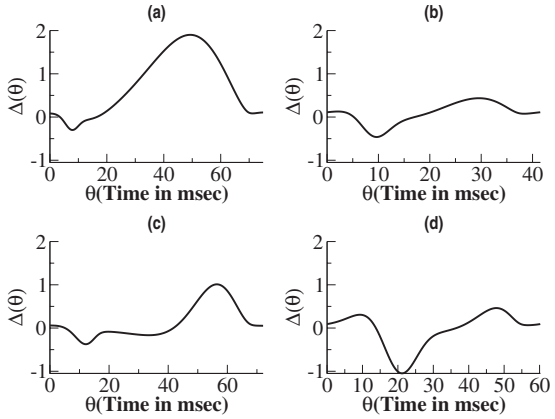

FIG. 6. Transformation of the PRC for the ML system in different frequency regimes. (a) ML system in type-I regime with an injected current of 50 μA (threshold around 40 μA). The PRC is almost completely type-I (b) PRC of ML system in *A* after the injected current is increased to 100 μA. The PRC is transformed to the type-II regime (c) ML system in type-II regime with an injected current of 120 μA (threshold around 100 μA). The PRC is type-II (d) transformation of PRC in *C* upon increasing injected current to 220 μA.

models, thus, it is important to understand the behavior of LIF neurons in a stochastic synchronization paradigm. In order to derive the order parameter for two LIF neurons we first obtained the PRC using the adjoint method. Briefly, if

$$\frac{dX}{dt} = F(X)$$

is a differential system in R^n and $X_0(t)$ is its T-periodic limit-cycle solution, then $x=X_0(t)$ is a point on the limit cycle at time(phase) t. The PRC is given by the function $Z(\phi)$, where

$$Z(\phi) = \nabla_X(\Theta(X_0(\phi))),$$

and $\Theta(x)$ is the phase function that relates a point on the limit cycle to its phase ϕ and is defined as

$$\Theta(X_0(\phi)) = \phi. \tag{13}$$

Differentiating Eq. (13) with respect to ϕ gives a relation between the PRC and $F(X)$,

$$Z(\phi)^T \frac{dX_0}{d\phi} = 1.$$

We derived the PRC for the LIF using the above formulation. Since we are in one dimension, this implies

$$Z(\phi) = \frac{1}{\frac{dX_0}{d\phi}}.$$

The LIF in its most general form is given as

$$\frac{dV}{dt} = -V + I. \tag{14}$$

Solving Eq. (14) we get

$$V(t) = I - Ie^{-t}. \tag{15}$$

The PRC is obtained by taking the reciprocal of the derivative of Eq. (15) with respect to t. Therefore,

$$Z(\phi) = \frac{e^{\phi}}{I}.$$

We calculated the autocorrelation function $h(x)$ of the PRC as follows:

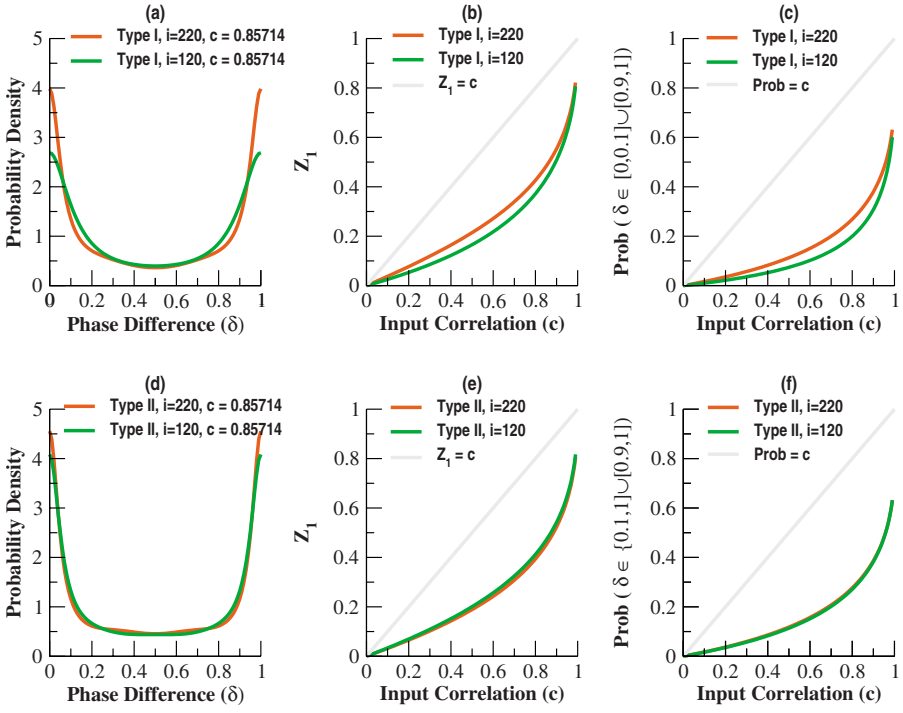

FIG. 7. (Color online) Simulations showing the effect of firing frequency on stochastic synchrony in type-I and type-II Morris-Lecar systems. The different input currents were $I=50,100$ for type I and $I=120,220$ for type II, $q=0.75$ for (a) and (d).

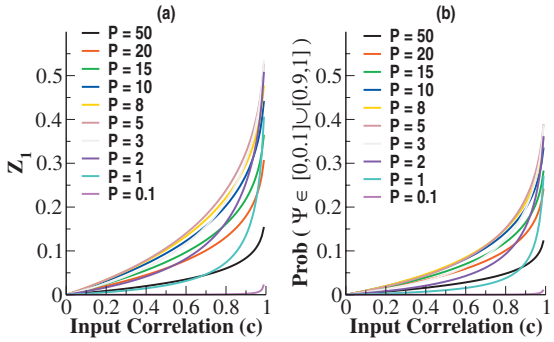

FIG. 8. (Color) Comparison of the order parameter obtained using an LIF neuron at different firing frequencies. Numbers indicate the time period between two successive spikes, $q \in [0,1)$.

$$h(x) = \int_0^{P-x} e^y e^{x+y} dy + \int_{P-x}^{P} e^y e^{x+y-P} dy$$

$$= \frac{1}{2}[e^{P-x}(e^P - 1) + e^x(e^P - 1)].$$

For calculating the order parameter for different periods we used the following simplifications:

$$H(x) = \frac{h(x)}{h(0)} = \frac{e^{P-x} + e^x}{e^P + 1}. \tag{16}$$

In order to parametrize the phase x we replace it with sP, where $s \in [0,1]$ and we can write Eq. (16) as

$$H(s,P) = \frac{e^{-Ps} + e^{P(s-1)}}{1 + e^{-P}}. \tag{17}$$

Using this we calculated the order parameter for different periods in Fig. 8. It can be observed that the order parameter is a nonmonotonic function of the period of oscillation. We plot the order parameter as a function of period for $q=0.75$ in Fig. 9. The position of the maxima of the order parameter curves depend on the period of oscillation. We show the order parameter obtained for a range of values for q and P in Fig. 10.

The Wang-Buzsaki model is a commonly used model for cortical interneurons [34]. It has a very wide range of frequencies and thus we investigated how this model is able to synchronize under a stochastic synchronization paradigm at

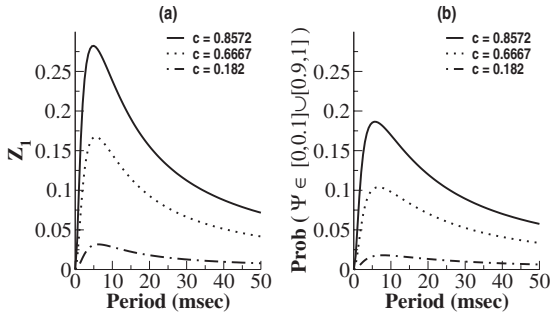

FIG. 9. Comparison of the order parameter obtained using LIF neurons at different periods at $q=0.75$, $c=0.857\,14$.

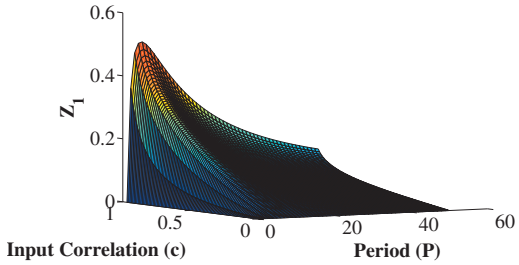

FIG. 10. (Color) Order parameter obtained from LIF neurons over a range of $q \in [0,1)$ and $P \in (0,50]$.

different frequencies. The adjoint was numerically calculated at different frequencies and the slope of the generalized order parameter with respect to input correlation was calculated as given in Eq. (12) and plotted in Fig. 11. It can be seen that the rate of change for the generalized order parameter has a sublinear relationship with respect to input correlation c, through almost the entire range of the neuron's firing frequency except possibly at the neuron's highest firing frequency where it reaches a value of 1, hence becoming linear. Additionally, this rate of change of the generalized order parameter with respect to the input correlation c, has a nonmonotonic relationship with respect to the firing frequency of the neuron wherein, in the lower frequency range it decreases from a value 0.5, close to 0 Hz to about 0.29 at around 33 Hz and then increases up to a value of 0.75 at around 400 Hz followed by a rapid increase to a value of 1 at the neuron's highest firing frequency around 500 Hz.

IV. DISCUSSION

In this work, we analyzed a system of identical, uncoupled limit-cycle oscillators receiving weak, partially correlated, Poisson distributed inputs. We derived an expression (9) for the probability density function of the phase difference between the two oscillators. Numerical simulations of Eq. (9) suggest a relative independence of the phase distribution with respect to the input rates at moderate to high input correlation values (Fig. 1) and weak inputs (Fig. 2). Thus we analyzed Eq. (9) under the assumption of low rates, which makes it possible to gain an intuitive understanding of

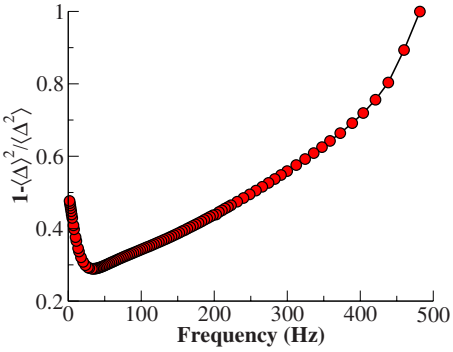

FIG. 11. (Color online) Slope for the generalized order parameter and input correlation dependence from the Wang-Buzsaki model over a range of firing frequencies.

the mechanism of PRC-shape dependent stochastic synchrony. Our results suggest that the shape of the PRC is crucial in controlling the magnitude of stochastic synchrony realized by the system.

By adopting circular variance as a measure of synchrony we show that type-II PRCs tend to show higher synchrony than type-I PRCs at all values of input correlation (Fig. 4). This result is also reflected identically in another measure of synchrony where we simply integrate the probability density between arbitrary upper and lower limits around zero. These results taken together suggest that the phase differences for oscillators with type-II PRCs are more densely clustered around zero compared to systems with type-I PRCs, which show longer tails. In other words, systems with type-II PRCs spend more time close to each other than those with type-I PRCs. We also show that the generalized order parameter, which is simply the sum of the correlations between the phase distribution function and all modes of cosine, is linear in the input correlation, for weak correlations.

In real neurons the shape of the PRC can be modulated by the firing frequency [13]. This modulation is mediated by slow adaptation processes, mainly slow potassium currents, which increase with an increase in firing frequency. But this increase in the slow potassium current also decreases the fractional contribution of the transient potassium currents at the start of the interspike interval (ISI), which causes an otherwise skewed PRC at moderate firing frequencies to become less skewed at higher frequencies. Our investigation suggests that synchronization is affected by firing frequency and decreases at higher frequencies (Fig. 5). That this difference in synchronization is observed without the change in the membership of the PRC (type I at both frequencies) only solidifies the role of subtle differences in the shape of PRC, in this case the degree of skewness, in dictating the system's propensity for undergoing stochastic synchronization.

In light of the above results, we investigated a system whose PRC undergoes substantial modulation in shape and changes membership at higher frequencies. Our results from simulations using the Morris-Lecar model show that stochastic synchrony increases with firing frequency as the PRC changes from a type I to type II. In contrast, when the system starts out in a type-II regime, the change in the circular variance due to an increase in firing frequency is minimal. A recent study, set in a similar setting, has shown that the output correlation of spike counts between LIF neurons increases with firing frequency [35]. Our results show a nonmonotonic relationship between circular variance of the phase differences and firing frequency. The circular variance of the phase difference does decrease with an increase in firing frequency but only up to a point beyond which it increases with frequency. We also note that the LIF has a type-I PRC at all firing frequencies. At this point the interrelationship between these different measures is unclear. A similar firing rate dependence was also observed for the Wang-Buzsaki model. The relationship between the slope of the generalized order parameter with respect to input correlation (12) and the firing rate was nonmonotonic Fig. 11, hence the relative increase in the generalized order parameter with respect to input correlation will be determined by the frequency of firing, similar to the observations in LIF. Such a firing rate dependent spike-time cross correlation has been reported in a recent study [36] (Fig. 8).

Our results suggest a strong effect of the shape of PRC on the synchronization properties of the cell. The shape of the PRC is determined by the variety of ion channels that define the dynamical behavior of a neuron. The relative contribution to membrane voltage of these ion channels depends on the firing rate of the neuron. We have described a mechanism by which these interactions might occur and finally be reflected in the spike-time correlation of general oscillator systems.

ACKNOWLEDGMENTS

We gratefully acknowledge support by NSF, as well as the discussions with Brent Doiron.

APPENDIX A: INPUT CORRELATION

Consider a Poisson process with rate r. For each spike let c be the probability that an oscillator receives that particular spike. The effective rate of the Poisson process for the neuron is just cr. Consider a pair of neurons. The probability that they both receive the given spike is c^2 and the probability that one receives a spike and the other does not is $c(1-c)$. Thus, c^2 is the fraction of shared inputs and c is the correlation of the inputs. $(1-c)^2$ is the probability that neither receives an input. For our problem, as the oscillators are identical, if neither receives input, then their phase difference remains the same until the next input comes in. Thus, the only cases in which an event occurs that changes the phases are those in which at least one oscillator receives an input. The fraction of relevant events (those in which at least one oscillator gets an input) with shared inputs is $c^2/(1-(1-c)^2)=c/(2-c)$. Recalling that q is the fraction of shared inputs, we see that $q=c/(2-c)$ or, $c=2q/(1+q)$. Thus, the quantity $2q/(1+q)$ is the input correlation.

APPENDIX B: INVARIANT DENSITY

The invariant density $\varphi(x)$ satisfies

$$\varphi(x) = \frac{1-q}{2}\int_0^1 Q(x-y)\varphi(y)dy + \frac{1+q}{2}\int_0^1 Q(x-y-\epsilon\Delta(y))\varphi(y)dy.$$

Here $Q(x)$ is the interspike interval or the waiting time density for a Poisson distribution with rate r modulo 1,

$$Q(x) = \frac{re^{-rx}}{1-e^{-r}}.$$

For $\epsilon=0$, $\varphi(x)=1$, so we expand in terms of ϵ to get the next order: $\varphi(x)=1+\epsilon\varphi_1(x)+\cdots$. The next order equation is

$$\varphi_1(x) = \int_0^1 Q(x-y)\varphi_1(y) - \frac{1+q}{2}\int_0^1 Q(x-y)\Delta'(y)dy,$$

along with the condition that the mean value of $\varphi_1(x)$ is zero [since the integral $\varphi(x)$ must be one for normalization]. For

general $Q(x)$ we can solve for $\varphi_1(x)$ by using a Fourier expansion. Specifically, write

$$\varphi_1(x) = \sum_n b_n e^{2\pi i n x},$$

$$Q(x) = \sum_n q_n e^{2\pi i n x},$$

$$\Delta(x) = \sum_n d_n e^{2\pi i n x}.$$

We must then have

$$b_n = -\frac{1+q}{2}\frac{2\pi i n q_n}{1-q_n} d_n.$$

For a Poisson process with rate r,

$$q_n = \frac{r}{r + 2\pi i n},$$

so that

$$b_n = -r\frac{1+q}{2} d_n,$$

as long as $n \neq 0$. For $n=0$, $b_0=0$ since the next order terms must have zero mean. Thus,

$$\varphi_1(x) = -r\frac{1+q}{2}(\Delta(x) - \int_0^1 \Delta(x)dx).$$

APPENDIX C: ORDER PARAMETERS

Consider the order parameters,

$$z_j = \int_0^1 p(y)\cos 2\pi j y \, dy, \quad j \geq 1.$$

If $p(x)$ is uniform, then each of these vanishes and if $p(x)$ is a delta function, then $z_j=1$. Consider the sum of these order parameters as a measure of the synchrony in all modes as follows:

$$Z = \theta \lim_{N\to\infty} \sum_{j=0}^{N} z_j - 1.$$

We have included z_0 in the sum and subtracted 1 from the total to compensate. Now, we formally rearrange the sum

$$Z = \int_0^1 p(x)\left[\lim_{N\to\infty} \sum_{j=1}^{N} \cos 2\pi j x\right] dx - 1.$$

The sum in the brackets forms a "delta sequence" (that is, in the limit, this sum goes to a Dirac delta function) (cf. [37]). Thus, $Z=p(0)-1$, exactly as derived above. For this reason, we treat $p(0)-1$, a generalized order parameter, as a measure of the local synchrony and correlation.

APPENDIX D: MODEL EQUATIONS

1. Morris-Lecar model

$$C_m\frac{dV}{dt} = g_L(V_L - V) + g_K w(V_K - V) + g_{Ca} m_\infty(v_{Ca} - V) + I,$$

$$\frac{dw}{dt} = \lambda_w(w_\infty - w),$$

$$m_\infty(V) = 0.5(1 + \tanh((V - V_1)/V_2)),$$

$$w_\infty(V) = 0.5(1 + \tanh((V - V_3)/V_4)),$$

$$\lambda_w(\phi, V) = \phi \cosh(0.5(V - V_3)/(V_4)).$$

For a type-II model, $V_K=-84$, $V_L=-60$, $V_Ca=120$, $g_K=8$, $g_L=2$, $g_{Ca}=4$, $C_m=20$, $V_1=-1.2$, $V_2=18$, $V_3=2$, $V_4=30$, $\phi=0.04$. For a type-I model we changed the following parameters: $V_3=12$, $V_4=17$, $\phi=0.0667$.

2. Wang-Buzsaki model

$$C_m\frac{dV}{dt} = g_L(V_L - V) + g_{Na} m_\infty^3 h(V_{Na} - V) + g_K(n^4)(V_K - V) + I,$$

$$m_\infty = a_m/(a_m + b_m),$$

$$a_m(V) = -0.1(V + 35)/(\exp(-0.1(V + 35)) - 1),$$

$$b_m(V) = 4\exp(-(V + 60)/18),$$

$$\frac{dh}{dt} = \phi(a_h(V)(1 - h) - b_h(V)h),$$

$$a_h(V) = 0.07\exp(-(V + 58)/20),$$

$$b_h(V) = 1/(\exp(-0.1(V + 28)) + 1),$$

$$\frac{dn}{dt} = \phi(a_n(V)(1 - n) - b_n(V)n),$$

$$a_n(V) = -0.01(V + 34)/(\exp(-0.1(V + 34)) - 1),$$

$$b_n(V) = 0.125\exp(-(V + 44)/80),$$

$$C_m = 1, \quad g_L = 0.1, \quad V_L = -65, \quad g_{Na} = 35, \quad V_{Na} = 55,$$

$$\phi = 5, \quad g_K = 9, \quad V_K = -90.$$

[1] A. Pikovsky, Radiophys. Quantum Electron. **27**, 576 (1984).
[2] J.-N. Teramae and D. Tanaka, Phys. Rev. Lett. **93**, 204103 (2004).
[3] D. S. Goldobin and A. Pikovsky, Phys. Rev. E **71**, 045201 (2005).
[4] D. Hong, W. M. Saidel, S. Man, and J. V. Martin, J. Theor. Biol. **245**, 726 (2007).
[5] K. Yoshimura, I. Valiusaityte, and P. Davis, Phys. Rev. E **75**, 026208 (2007).
[6] C. Li, L. Chen, and K. Aihara, BMC Syst. Biol. **1**, 6 (2007).
[7] K. Park, Y.-C. Lai, S. Krishnamoorthy, and A. Kandangath, Chaos **17**, 013105 (2007).
[8] Q. Li and Y. Wang, Biophys. Chem. **129**, 23 (2007).
[9] H. Nakao, K. Arai, and Y. Kawamura, Phys. Rev. Lett. **98**, 184101 (2007).
[10] R. F. Galan, N. Fourcaud-Trocme, G. B. Ermentrout, and N. N. Urban, J. Neurosci. **26**, 3646 (2006).
[11] J. Rinzel and G. Ermentrout, *Methods in Neuronal Modeling* (MIT Press, Cambridge, MA, 1989).
[12] B. Ermentrout, M. Pascal, and B. Gutkin, Neural Comput. **13**, 1285 (2001).
[13] B. S. Gutkin, G. B. Ermentrout, and A. D. Reyes, J. Neurophysiol. **94**, 1623 (2005).
[14] D. Hansel, G. Mato, and C. Meunier, Neural Comput. **7**, 307 (1995).
[15] E. Brown, J. Moehlis, and P. Holmes, Neural Comput. **16**, 673 (2004).
[16] B. Ermentrout, Neural Comput. **8**, 979 (1996).
[17] D. Golomb and D. Hansel, Neural Comput. **12**, 1095 (2000).
[18] B. Ermentrout and N. Kopell, *Handbook of Dynamical Systems* (Elsevier, Amsterdam, 2000).
[19] R. F. Galan, G. B. Ermentrout, and N. N. Urban, Neurocomputing **70**, 2102 (2007).
[20] J. A. Goldberg, C. A. Deister, and C. J. Wilson, J. Neurophysiol. **97**, 208 (2007).
[21] J. G. Mancilla, T. J. Lewis, D. J. Pinto, J. Rinzel, and B. W. Connors, J. Neurosci. **27**, 2058 (2007).
[22] T. Netoff (private communication).
[23] T. Tateno and H. P. C. Robinson, Biosystems **89**, 110 (2007).
[24] T. Tateno and H. P. C. Robinson, Biophys. J. **92**, 683 (2007).
[25] R. F. Galan, G. B. Ermentrout, and N. N. Urban, Phys. Rev. E **76**, 056110 (2007).
[26] Y. Tsubo, M. Takada, A. D. Reyes, and T. Fukai, Eur. J. Neurosci. **25**, 3429 (2007).
[27] Y. Kuramoto, *Chemical Oscillations, Waves and Turbulence* (Springer Verlag, New York, 1984).
[28] G. B. Ermentrout, *Simulating, Analyzing, and Animating Dynamical Systems: A Guide to XPPAUT for Researchers and Students* (SIAM, Philadelphia, 2002).
[29] A. Lasota and M. C. Mackey, *Differential Equations with Applications to Biology (Fields Institute Communications)* (American Mathematical Society, Providence, RI, 1999).
[30] H. Nakao, K.-S. Arai, K. Nagai, Y. Tsubo, and Y. Kuramoto, Phys. Rev. E **72**, 026220 (2005).
[31] B. Ermentrout and D. Saunders, J. Comput. Neurosci. **20**, 179 (2006).
[32] F. H. Allen and O. Johnson, Acta Crystallogr. B **47**, 62 (1991).
[33] B. Pfeuty, G. Mato, D. Golomb, and D. Hansel, Neural Comput. **17**, 633 (2005).
[34] X. J. Wang and G. Buzsaki, J. Neurosci. **16**, 6402 (1996).
[35] J. de la Rocha, B. Doiron, E. Shea-Brown, K. Josic, and A. Reyes, Nature (London) **448**, 802 (2007).
[36] A. Kohn and M. A. Smith, J. Neurosci. **25**, 3661 (2005).
[37] J. P. Keener, *Principles of Applied Mathematics: Transformation and Approximation* (Westview Press, Cambridge, MA, 2000).